Feeling blue

Gardner, Dominic; James, Matthew; Wright, Sophie; Williams, Jacob; Baldwin, Olivia ; Ball, Tom; Cooper, Emily; Monk, Catherine; Driscoll, Lizzie; Slater, Peter

DOI:
https://doi.org/10.26434/chemrxiv-2023-spq6s

Document Version
Peer reviewed version

Citation for published version (Harvard):
Gardner, D, James, M, Wright, S, Williams, J, Baldwin, O, Ball, T, Cooper, E, Monk, C, Driscoll, L & Slater, P 2023 'Feeling blue: utilising cation ordering to engineer the colour of apatite pigments' ChemRxiv. https://doi.org/10.26434/chemrxiv-2023-spq6s

Feeling blue: utilising cation ordering to engineer the colour of apatite pigments

D. J. Gardner*, M. S. James*, S. L. Wright, J. R. Williams, O. L. Baldwin, T. Ball, E. Cooper, C. E. Monk, E. H. Driscoll, P. R. Slater*

School of Chemistry, University of Birmingham, Birmingham, B15 2TT, United Kingdom

Abstract

Manganese doped chlorapatite compounds have attracted interest as inorganic pigments due to their vivid colours. In this paper, we investigate the effect of Sr incorporation in the turquoise pigment $Ba_{10}(MnO_4)(PO_4)_5Cl_2$. on the structure and optical properties. The results show a turquoise colour throughout the series studied, except for a single compound, $Ba_6Sr_4(MnO_4)(PO_4)_5Cl_2$ which exhibits an intense blue hue. The colour change is explained by Ba/Sr cation ordering in the apatite structure, with this composition corresponding to complete occupation of the A1 site by Sr and the A2 site by Ba, and similar results are also observed for the related manganese doped bromoapatite system. The unique blue colour for these cation ordered compositions illustrates the potential to control the colour of apatite pigments through exploiting cation site preferences, while its' low cost represents a key advantage compared to recently reported blue $YIn_{1-x}Mn_xO_3$ pigments.

Keywords: apatite, cation ordering, blue pigment

Introduction

The discovery of novel blue ceramic pigments has attracted significant interest, since currently, some of the most used commercial pigments contain cobalt, e.g. cobalt aluminate spinel ($CoAl_2O_4$) and cobalt (II) stannate (Co_2SnO_4) [1-5]. Due to the toxicity, limited resources of cobalt raw materials and their increasing use in energy materials, new cheap, durable, and low toxicity blue pigments that avoid the use of cobalt are needed [6-7].

Recent research on $YIn_{1-x}Mn_xO_3$ has illustrated the potential to prepare cobalt-free blue ceramic pigments with the colour due to Mn^{3+} in trigonal bipyramidal coordination in this compound [8-13]. The vivid blue colour, low toxicity, and thermal stability have led to this pigment being recently approved for commercial use. The $YIn_{1-x}Mn_xO_3$ series has also been shown to have excellent near-infrared reflectance and show potential as cool pigments for use to reflect solar heat such as roofing materials [14]. However, the cost associated with indium-based precursors causes an issue with these compositions.

Other Mn-containing compounds have also been studied for their colour such as brownmillerite and apatite type structures, although these colours tend to range from turquoise to dark green depending on manganese content [15-19]. The apatite material has the general formula $A_{10}(MO_4)_6X_2$ where typically A = Ca, Sr, Ba or La, M =Si, Ge, P or V and X = O, OH or halides [20-23]. The apatite structure can be classed as an $A_4(MO_4)_6$ framework which contains A cations (A1 site) in trigonal metaprisms that are corner-linked with the tetrahedral MO_4 units. The remaining A cations (A2 site) and X anions are located within the cavities of this framework (Figure 1). The apatite structure shows excellent flexibility for doping on the different sites, and such doping strategies can lead to a variety of properties, such as high ionic conductivity and luminescence [23-25]. The use of different dopants can also change the colour of apatites. Previously, apatite pigments have been made by doping with transition metals, with the colours observed attributed to d-d transitions or to charge transfer bands. One such example is the doping of Mn^{5+} which can be doped onto the tetrahedral site and is noted to produce an intense turquoise colour [19].

Despite the interest in this pigment material, there have been no studies of the effect of substitution of Ba for Sr, which offers the ability to examine how the different site preferences of Ba and Sr affect the colour of the resultant apatite. Consequently, through a third year undergraduate mini-lab project, we investigated the effect of Sr doping in $Ba_{10}(MnO_4)(PO4)_5Cl_2$. The results show a unique member of the solid solution series, $Ba_6Sr_4(MnO_4)(PO_4)_5Cl_2$, which has a vivid blue colour attributed to this composition having perfect ordering between the Sr/Ba on the A1/A2 sites, and similar results are also shown for the Br analogue, $Ba_6Sr_4(MnO_4)(PO_4)_5Br_2$.

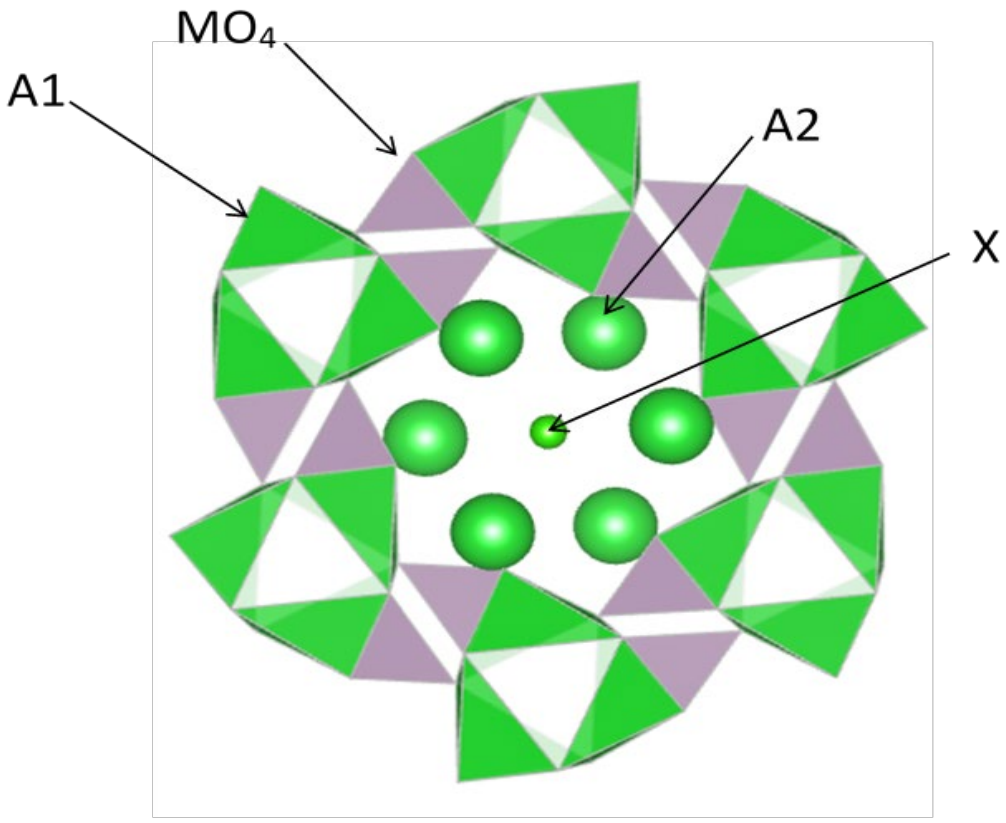

Figure 1: Crystal Structure of $A_{10}(MO_4)_6X_2$ with highlighted A1, A2, MO_4, and X sites.

Experimental

High purity $SrCO_3$, $BaCO_3$, MnO_2, $(NH_4)H_2PO_4$, $BaCl_2$ were used to prepare $Ba_{10-x}Sr_x(MnO_4)(PO_4)_5Cl_2$ ($0 \leq x \leq 5$) samples. Stoichiometric mixtures of the powders were intimately ground and initially heated to 900 °C (10 °C min^{-1}) for 12 hours. Samples were then reground and reheated to 950-1150 °C (10 °C min^{-1}) for a further 12-24 hours, depending on the apatite composition. Similar conditions were used to prepare the bromoapatite samples, with $BaBr_2$ used instead of $BaCl_2$.

Powder X-ray diffraction (PXRD) data were collected to determine phase purity, unit cell parameters and for preliminary structure refinement. PXRD patterns (10 to 90° 2θ) were collected on a Panalytical Empyrean diffractometer equipped with a Pixcel 2D detector (Cu Kα radiation). The GSAS-II suite of programs was used for structure refinement (26)

FT-IR Spectroscopy measurements were performed using a Bruker Alpha II FTIR-Spectrometer with the platinum ATR attachment.

Colour coordinates were initially obtained via RGB measurements from colour photos and further confirmed via measurements using a BELEY 8mm MODEL WR-10 QC portable colourimeter.

Results and Discussion

All $Ba_{10-x}Sr_x(MnO_4)(PO_4)_5Cl_2$ ($0 \leq x \leq 5$) samples investigated were shown to form a single phase apatite material (see supplementary info: Fig SI-1). The structures (space group of *P 6₃ / m)* were refined using the Rietveld refinement method. The unit cell parameters (Figure 2), showed the expected reduction in unit cell size on increasing Sr content, as expected due to smaller size of Sr^{2+} compared to Ba^{2+}. The refined lattice parameters and the Rietveld refinement goodness of fit parameters are presented in Table 1. In the Rietveld refinement, the manganese and phosphorous were all placed in the MO_4 tetrahedral sites using the expected stoichiometric amounts. In line with previous literature studies on cation partitioning within apatite structures which have suggested large ions preferentially favour the A2 sites, with small cations the A1 sites [27], the refinements here confirmed this preference with Sr favouring the A1 site and Ba the A2 site. Figure 3 shows a representative Rietveld refinement profile fit for the x=4 sample, $Ba_6Sr_4(MnO_4)(PO_4)_5Cl_2$ structure. For this $Ba_6Sr_4(MnO_4)(PO_4)_5Cl_2$ composition, there is complete ordering with Sr and Ba fully occupying the A1 and A2 sites respectively (the structural parameters for this phase are shown in Table 2).

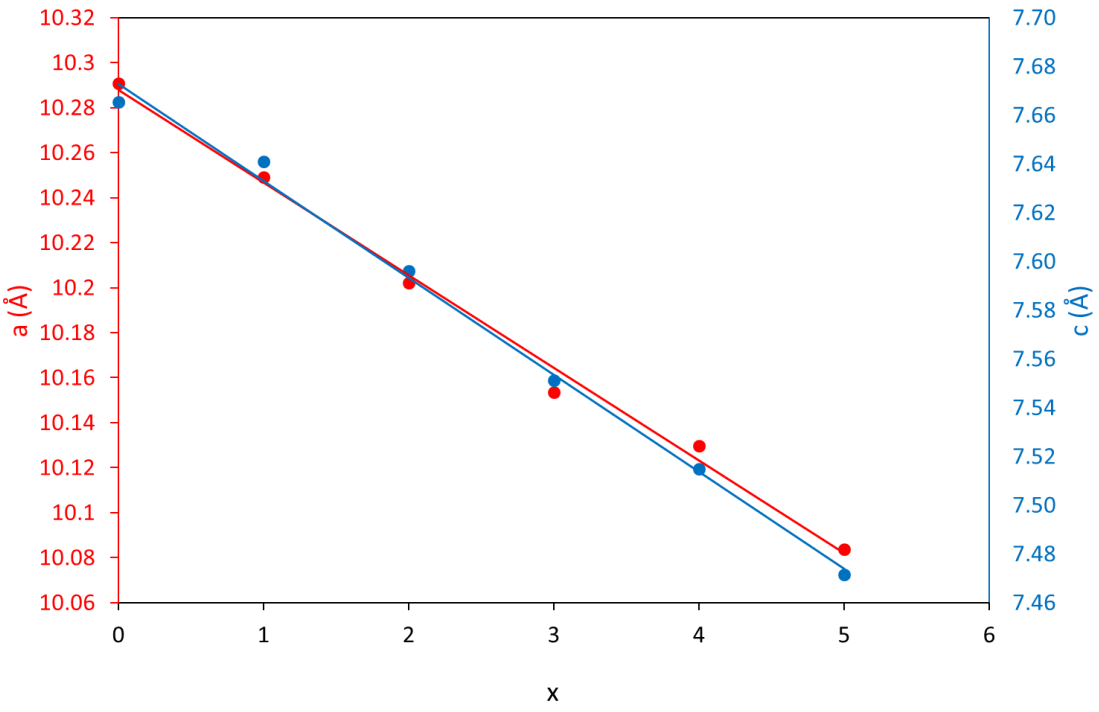

Figure 2a: Variation of unit cell parameters with Sr content for $Ba_{10-x}Sr_x(MnO_4)(PO_4)_5Cl_2$

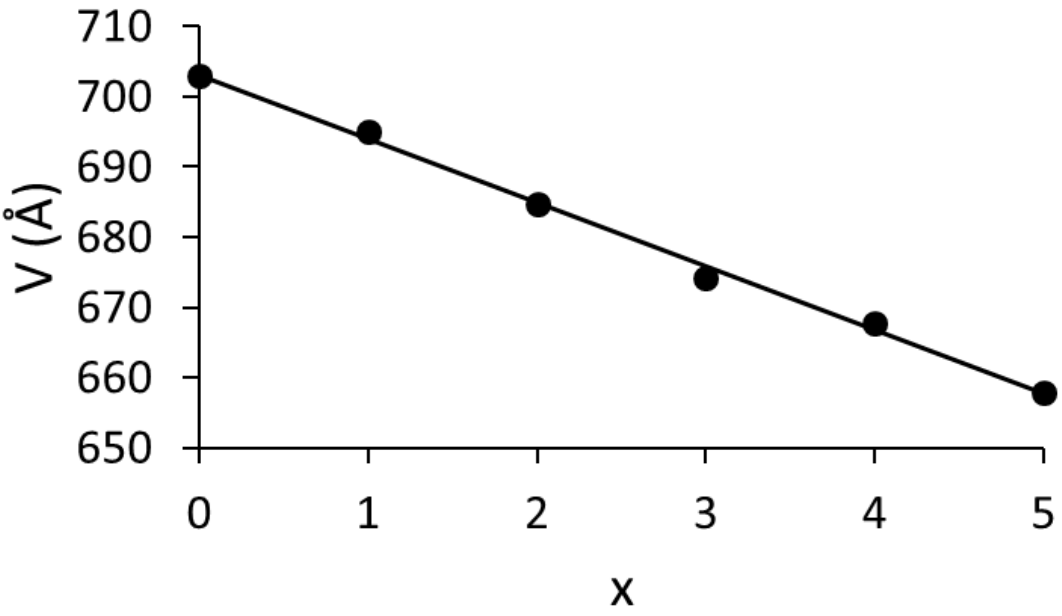

Figure 2b: Variation of cell volume with Sr content for $Ba_{10-x}Sr_x(MnO_4)(PO_4)_5Cl_2$

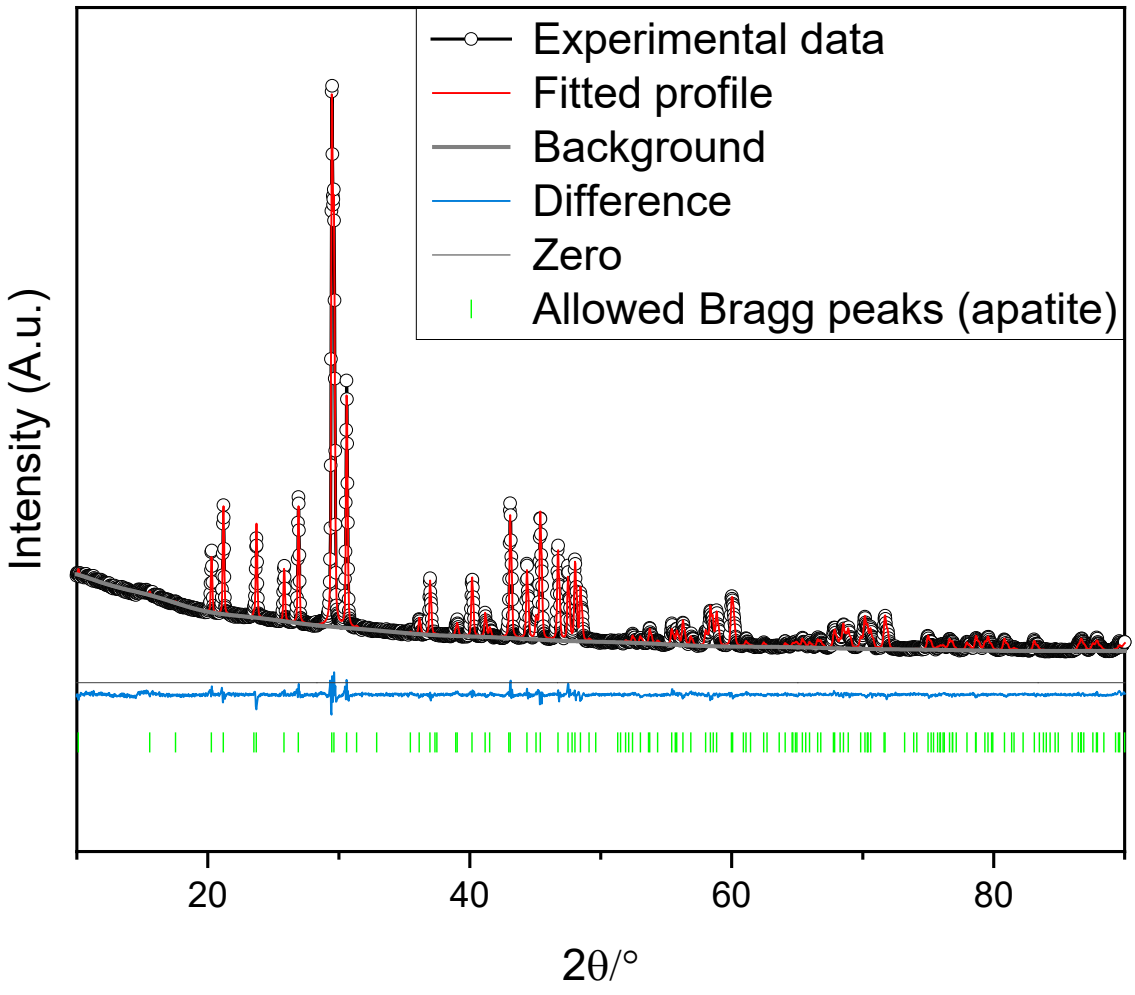

Figure 3: Representative Rietveld profile fit: $Ba_6Sr_4(PO_4)_5(MnO_4)Cl_2$ (x=4). wR = 2.319%.

Table 1: Cell parameters and goodness of fit values for Rietveld refinement of $Ba_{10-x}Sr_x(MnO_4)(PO_4)_5Cl_2$

x	a (Å)	c (Å)	Unit Cell Volume (Å^3)	WRp	Rp	χ^2
0	10.2906(7)	7.6653(3)	702.99(6)	7.17	4.63	1.55
1	10.2492(8)	7.6409(9)	695.13(1)	5.99	4.47	1.34
2	10.2023(1)	7.5960(2)	684.72(3)	5.80	3.67	1.58
3	10.1536(5)	7.5512(7)	674.21(9)	5.96	3.47	1.72
4	10.1278(3)	7.5145(8)	667.52(2)	2.32	1.25	1.85
5	10.0836(7)	7.4714(1)	657.92(1)	5.73	2.88	1.99

Table 2: Structural parameters for $Ba_6Sr_4(MnO_4)(PO_4)_5Cl_2$

Atoms	Wyckoff Position	x	y	Z	Occupancy	U_{iso} (Å^2)
Sr1	4f	0.6667	0.3333	-0.0002(6)	1.0000	0.0117(5)
Ba1	6h	0.2445(2)	0.9827(2)	0.2500	1.0000	0.0364(4)
Mn1	6h	0.4047(7)	0.3705(7)	0.2500	0.167	0.04(2)
P1	6h	0.4030(7)	0.3709(7)	0.2500	0.833	0.04(2)
Cl1	2b	0.0000	0.0000	0.02(3)	1.0000	0.05(2)
O1	6h	0.364(2)	0.494(1)	0.2500	1.0000	0.05(2)
O2	6h	0.587(2)	0.453(1)	0.2500	1.0000	0.05(2)
O3	12i	0.3546(7)	0.2746(9)	0.0741(9)	1.0000	0.05(2)

In addition to the collection of X-ray diffraction data, IR spectra were recorded for the samples (figure 4). The data were comparable to previous literature reports for apatite systems [26]. Peaks between 700-1100 cm^{-1} are attributed to the MO_4 tetrahedra, with the peaks around 1000 cm^{-1} associated with the PO_4^{3-} group vibrational modes (v_1 - symmetrical and v_3 - asymmetrical modes). All samples also have v_3 vibrational peaks associated with MnO_4^{3-} around 720 to 780 cm^{-1} consistent with literature values for such a moiety. (18) There is an observed shift of all vibrational modes to higher wavenumber on increasing the strontium content.

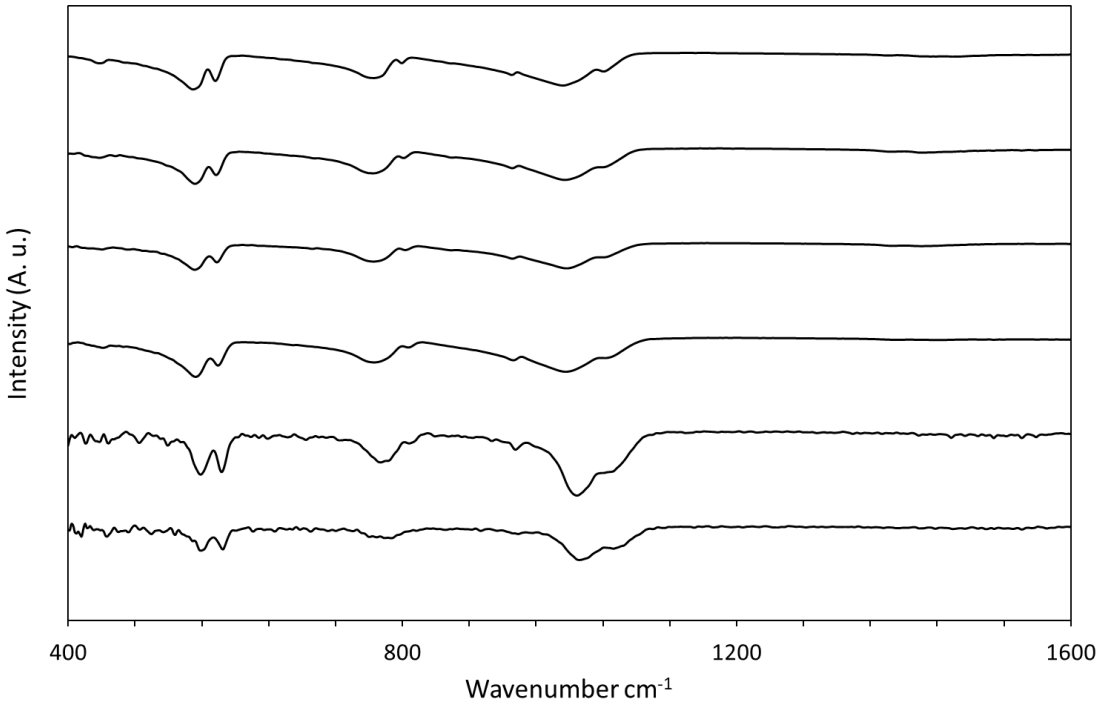

Figure 4: IR spectra for $Ba_{10-x}Sr_x(MnO_4)(PO_4)_5Cl_2$ phases from top to bottom: x= 0,1,2,3,4 and 5

Colour measurements

Previous studies of $Ba_{10}(MnO_4)(PO_4)_5Cl_2$ had reported a dark turquoise colour, and a similar colour was observed for our sample [18]. A similar dark turquoise colour was observed for the Sr doped samples, with the exception of $Ba_6Sr_4(MnO_4)(PO_4)_5Cl_2$, where a clearer blue hue was observed (figure 5). This particular sample has complete ordering of Sr/Ba in the A1/A2 sites, and thus highlights a key influence of cation ordering on the colour of the pigment. In this respect, computer modelling studies of the influence of the doping strategy/cation ordering on the electronic structure would be of interest for the compositions around this "sweet spot".

Figure 5: Colour image of $Ba_{10-x}Sr_x(MnO_4)(PO_4)_5Cl_2$ phases from left to right: x = 0, x = 1, x = 2, x = 3, x = 4 and x = 5

To characterise the colour of $Ba_{10-x}Sr_x(MnO_4)(PO_4)_5Cl_2$ solid solutions, the colour coordinates were measured (Figure 6). The results show that the a* and b* values are fairly consistent across the series except for $Ba_6Sr_4(MnO_4)(PO_4)_5Cl_2$, where a* increased and b* decreased compared to the other compositions within the series. These changes are consistent with the colour reflected in $Ba_6Sr_4(MnO_4)(PO_4)_5Cl_2$ being bluer and less green, hence a more vivid overall blue colour is observed for this sample.

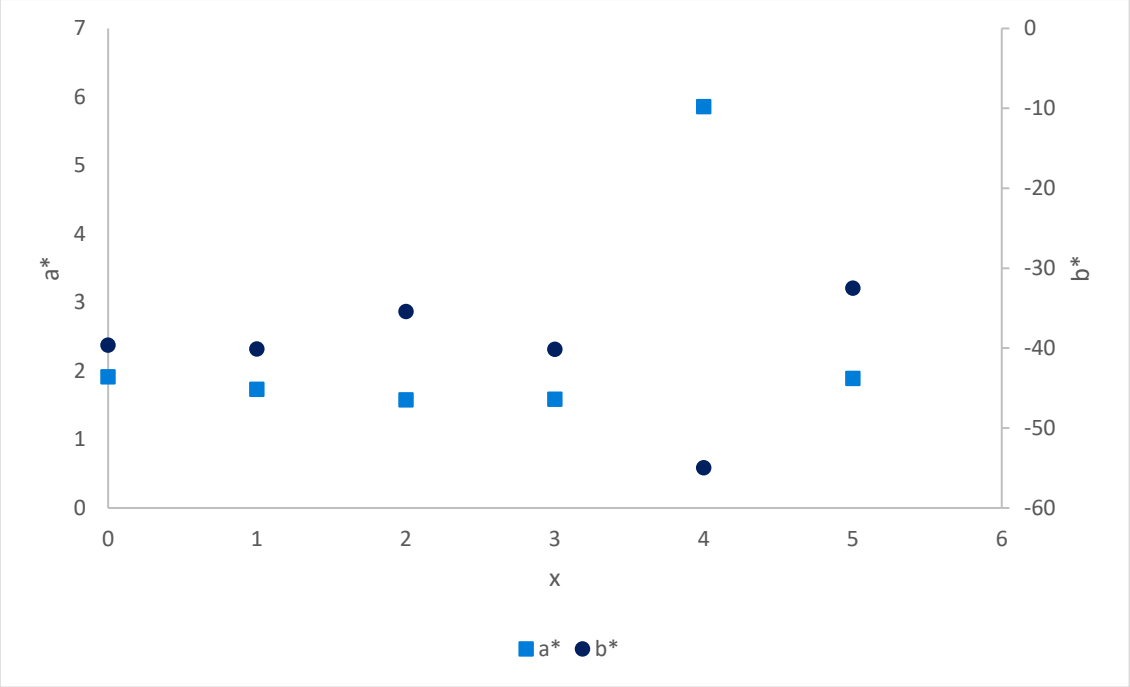

Figure 6: a*(responsible for a red (a*>0)/green(a*<0) components of colour), b*(responsible for a yellow (b*>0)/blue(b*<0) components of colour) parameters of samples as a function of Sr content (x) showing the significant change for the x=4 composition.

Thus, the work has shown the production of a new blue pigment for this cation ordered composition, $Ba_6Sr_4(MnO_4)(PO_4)_5Cl_2$, which is a significantly cheaper material to prepare than the previously reported $YIn_{1-x}Mn_xO_3$ series (associated with the high cost of indium). Therefore, this particular composition, $Ba_6Sr_4(MnO_4)(PO_4)_5Cl_2$ warrants further study for industrial applications. In this respect, a larger batch (≈40g) has been synthesised to show scalability of this material for potential industrial use applications with a similar colour being retained as in the smaller synthesis batch.

Further preliminary studies have shown that the related bromoapatite phase, $Ba_6Sr_4(PO_4)_5(MnO_4)Br_2$ can also be prepared; The XRD pattern of this phase indicates the formation of an apatite structure similar to the $Ba_6Sr_4(PO_4)_5(MnO_4)Cl_2$ system (figure 7). The colour of this pigment (figure 8) was a slightly paler blue with a hint of turquoise, hence the colour coordinates show increased amounts of green and lesser amounts of blue contributing to the overall colour seen (a* = -11.93, b* = -37.86).

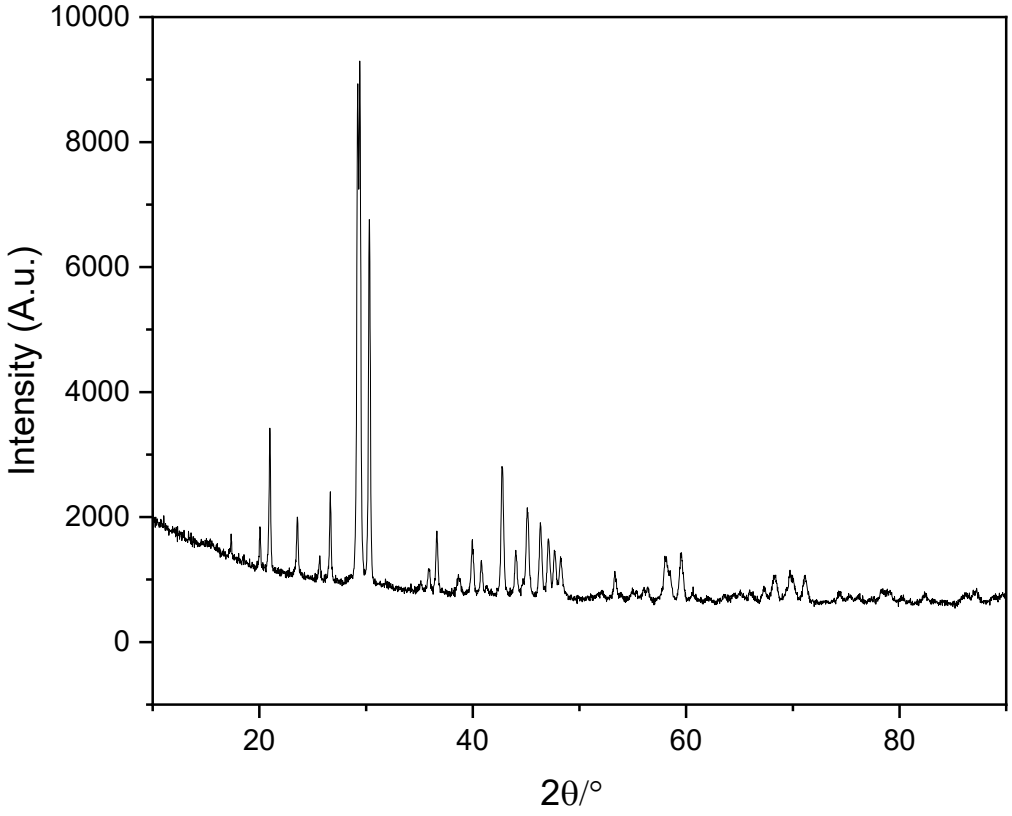

Figure 7: Powder X-Ray Diffraction pattern of $Ba_6Sr_4(MnO_4)(PO_4)_5Br_2$.

Figure 8: Colour Image of the $Ba_6Sr_4(PO_4)_5(MnO_4)Br_2$ pigment.

Conclusions

In this paper we have shown that Sr can be incorporated into $Ba_{10}(MnO_4)(PO_4)_5Cl_2$ resulting in the synthesis of new apatite pigments. All the pigments had a dark turquoise colour, with the exception of the composition, $Ba_6Sr_4(MnO_4)(PO_4)_5Cl_2$, which gave a more commercially desirable blue colour. The difference can be attributed to this latter phase showing complete Sr/Ba ordering over the A1/A2 sites, and the work highlights that cation ordering can be exploited to modify the colours of apatite pigments. The related $Ba_6Sr_4(PO_4)_5(MnO_4)Br_2$ blue pigment could also be prepared. Given that these materials are prepared from low-cost

precursors, they represent promising new blue pigments. Further studies are warranted to explore the local structural changes around the MnO_4 chromophore in order to rationalise the observed colour changes on Sr doping.

Acknowledgements

The authors acknowledge the University of Birmingham for their support (PhD studentship for MSJ). The authors also thank the Collaborative Teaching Laboratories (CTL) for the use of laboratory space, equipment and materials during the running of this experiment. Further acknowledgement is given Daniel Butler at the University of Birmingham for his help in performing the colour measurements and to Dr Joshua Deakin for his guidance on Rietveld refinements on GSAS-II.

Conflicts of Interest

There are no conflicts of interest to declare.

Author Contributions

Dominic Gardner: Conceptualisation, Data Curation, Formal Analysis, Investigation, Validation, Visualisation, Writing – original draft, Writing – review & editing.

Matthew James: Conceptualisation, Data Curation, Formal Analysis, Investigation, Visualisation, Writing – original draft.

Sophie Wright: Data Curation, Formal Analysis, Investigation, Visualisation, Writing – original draft.

Jacob Williams: Data Curation

Olivia Baldwin: Data Curation

Tom Ball: Data: Data Curation

Emily Cooper: Data Curation

Catherine Monk: Data Curation

Elizabeth Driscoll: Writing – review & editing.

Peter Slater: Conceptualisation, Investigation, Methodology, Project Administration, Resources, Supervision, Writing – original draft, Writing – review & editing.

References

1. A. Aguilar-Elguézabal, M. Román-Aguirre, L. D. L Torre-Sáenz, P. Pizá-Ruiz and M. Bocanegra-Bernal, *Ceram. Int.,* **43**(17), 15254-15257, (2017)
2. X. Peng, J. Chen, J. Yuan, N. Jin, J.Kang, Y. Hou and Q. Zhang, *Adv. Appl. Ceram,* **117,** 303-311, (2018)
3. X. Duan, M. Pen, F. Yu, D. Yuan, *J. Alloys. Compd.,* **509**(3)**,** 1079-1083, (2011)
4. M. Llusar, A. Forés, J. A. Badenes, J. Calbo, M. A. Tena and G. Monrós, *J. Eur. Cream.,* **21**(8), 1121-1130, (2001)

5. M. Llusar, A. Zielinkska, M. A. Tena, J. A. Badenes and G. Monrós, *J. Eur. Cream, **30**(9),* 1887-1896, (2010)
6. B. A. Duell, J.Li and M. A. Subramanian, *ACS Omega,* **4**, 22114-22118, (2019)
7. Y. F. Gomes, J. Li, K. F. Silva, A. A. G. Santiago, M. R. D. Bomio, C. A. Paskocimas, M. A Subramanian, F. V. Motta, *Ceram. Int.,* **44**(11), 11932-11939, (2018)
8. Y. Zhou, P. Jiang, J. Kuang, X. Yang, W. Cao, *Solid. State. Sci.,***81,** 8-11, (2018)
9. A. E. Smith, H. Mizoguchi, K. Delaney, N. A. Spaldin, A. W. Sleight and M. A. Subramanian, **131**(47), 17084-17086, (2009)
10. J. Li, M. A. Subramanian, *J. Solid. State. Chem.,* **272,** 9-20, (2019)
11. L. Liu, M. Li, K. Cui, Y. Wang, J. Kunag, W. Cao, *Solid. State. Sci.,* **113,** 106516, (2021)
12. A. Rosati, M. Fedel, S. Rossi, *J. Solid. State. Chem.,* **299,** 122176, (2021)
13. A. E. Smith, M. C. Comstock, M. A. Subramanian, *Dyes. Pigm.,* **133**, 214-221, (2016)
14. P. K. Thejus, K. V. Kriishnapriya, K. G. Nishanth, **219,** 110778, (2021)
15. G. Gramm, G. Fuhrmann, K. Ploner, S. Penner, H. Huppertz, *Mater. Adv.,* **1,** 2293-2299 (2020)
16. S. W. Kim, G. E. Sim, J. Y. Ock, J. H. Son, T. Hasegawa, K. Toda, D. S. Bae, *Dyes. Pigm.,* **139,** 344-348, (2017)
17. T-G Kim, S-J. Kim, C. C. Lin, R-S. Liu, T-S. Chan. S-J. Im, *J. Mater. Chem. C.,* **1,** 5843-5848*,* (2013)
18. E. A. Medina, J. Li, J. K. Stalick and M. A. Subramanian, *Solid. State. Sci.,* **52,** 97-105, (2016)
19. S.Laha, S. Tamilarasan, S. Natarajan, J. Gopalakrishnan, *Inorg Chem.,* **55,** 3508-2514 (2016)
20. V. V. Kharton, F. M. B. Marques, A. Atkinson, *Solid State Ion.,* **174,** 135-149, (2004),
21. P. M. Panchmatia, A. Orera, G. J. Rees, M. E. Smith, J. V. Hanna, P. R. Slater, M. S. Islam, *Angew. Chem. Int. Ed.,* **50** 9328-9333 (2011)
22. S. W. Thomas, M. S. James, M. P. Stockham, J. Deakin, A. Jarvis, P. R. Slater, *ECS Trans,* 103(1), 1885-1897 (2021)
23. A. Orera, P. R. Slater, *Chem, Mater* (2010), **22**(3), 675-690
24. P. R. Slater, J. E. H Sansom, J. R. Tolchard, *Chem. Rec.,* **4,** 373-384, (2004)
25. M. Czaja, S. Bodyl, P. Gluowski, Z. Mazurak, W. Strek, *J. Alloys. Compd.,* **451,** 290-292 (2004)
26. Y-Y. Wang, Y-X. Liu, H-H. Lu, R-Q. Yang, S-M. Yang, J. Solid State Chem, 2018, **261**, 53-61.
27. B. H. Toby, R. B. Von Dreele, *J. Appl. Crystl.,* **46**(2), 544-549 (2013)

28. S. C. Lim, T. Baikie, S. S. Pramana, R. Smith and T. J. White, *J. Solid State Chem.,* **184**(11), 2978-2986, (2011)

29. B. J. Corrie, J. F. Shin, S. Hull, K. S. Knight, M. C. Vlachou, J. V. Hanna and P. R. Slater, Dalton Trans., 2015, **45**, 121-133.

Feeling blue: utilising cation ordering to engineer the colour of apatite pigments

D. J. Gardner*, M. S. James*, S. L. Wright, J. R. Williams, O. L. Baldwin, T. Ball, E. Cooper, C. E. Monk, E. H. Driscoll, P. R. Slater*

School of Chemistry, University of Birmingham, Birmingham, B15 2TT, United Kingdom

Supporting Information

Additional X-ray diffraction patterns for the $Ba_{10-x}Sr_x(MnO_4)(PO_4)_5Cl_2$ series

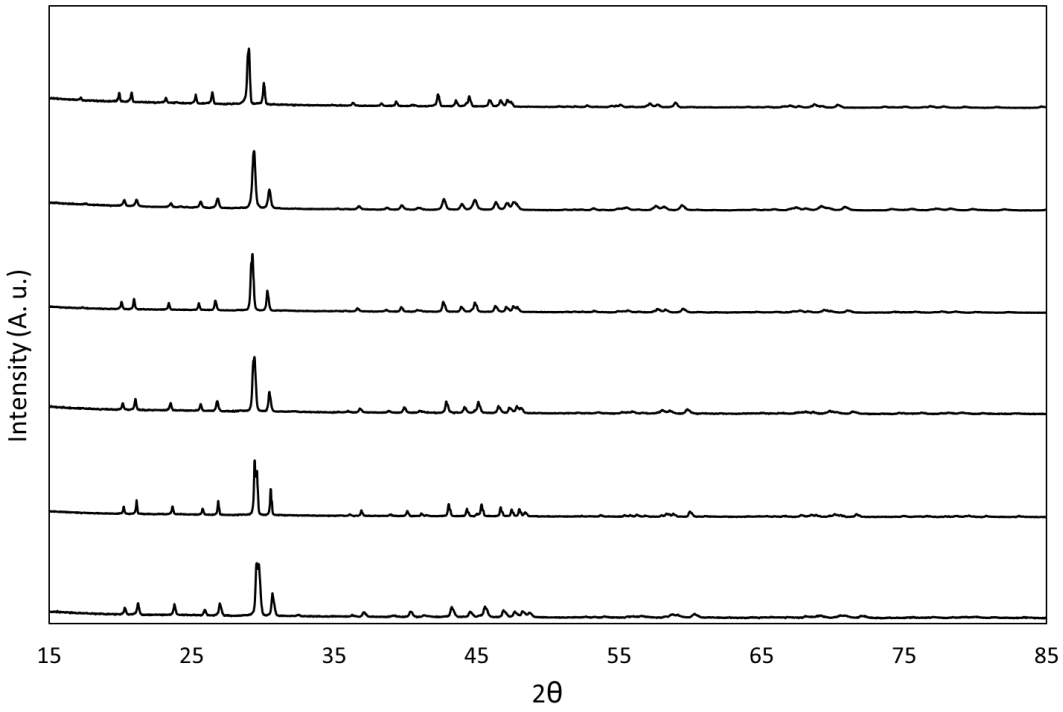

Figure SI-1: Powder X-ray diffraction pattern of $Ba_{10-x}Sr_x(MnO_4)(PO_4)_5Cl_2$ from top to bottom: x = 0,1,2,3,4 and 5